The American Journal of Pathology, Vol. 185, No. 5, May 2015

ELSEVIER

The American Journal of
PATHOLOGY
ajp.amjpathol.org

MUSCULOSKELETAL PATHOLOGY

Targeted Deletion of Collagen V in Tendons and Ligaments Results in a Classic Ehlers-Danlos Syndrome Joint Phenotype

Mei Sun,* Brianne K. Connizzo,† Sheila M. Adams,* Benjamin R. Freedman,† Richard J. Wenstrup,‡ Louis J. Soslowsky,† and David E. Birk*

From the Department of Molecular Pharmacology & Physiology, Morsani College of Medicine, University of South Florida, Tampa, Florida; the McKay Orthopedic Research Laboratory,† University of Pennsylvania, Philadelphia, Pennsylvania; and the Myriad Genetic Laboratories,‡ Salt Lake City, Utah*

Accepted for publication January 2, 2015.

Address correspondence to David E. Birk, Ph.D., Department of Molecular Pharmacology & Physiology, Morsani College of Medicine, University of South Florida, 12901 Bruce B. Downs Blvd., MDC8, Tampa, FL 33612-4799. E-mail: dbirk@health.usf.edu.

Collagen V mutations underlie classic Ehlers-Danlos syndrome, and joint hypermobility is an important clinical manifestation. We define the function of collagen V in tendons and ligaments, as well as the role of alterations in collagen V expression in the pathobiology in classic Ehlers-Danlos syndrome. A conditional *Col5a1*$^{flox/flox}$ mouse model was bred with Scleraxis-Cre mice to create a targeted tendon and ligament *Col5a1*-null mouse model, *Col5a1*$^{\Delta ten/\Delta ten}$. Targeting was specific, resulting in collagen V—null tendons and ligaments. *Col5a1*$^{\Delta ten/\Delta ten}$ mice demonstrated decreased body size, grip weakness, abnormal gait, joint laxity, and early-onset osteoarthritis. These gross changes were associated with abnormal fiber organization, as well as altered collagen fibril structure with increased fibril diameters and decreased fibril number that was more severe in a major joint stabilizing ligament, the anterior cruciate ligament (ACL), than in the flexor digitorum longus tendon. The ACL also had a higher collagen V content than did the flexor digitorum longus tendon. The collagen V—null ACL and flexor digitorum longus tendon both had significant alterations in mechanical properties, with ACL exhibiting more severe changes. The data demonstrate critical differential regulatory roles for collagen V in tendon and ligament structure and function and suggest that collagen V regulatory dysfunction is associated with an abnormal joint phenotype, similar to the hypermobility phenotype in classic Ehlers-Danlos syndrome. *(Am J Pathol 2015, 185: 1436—1447; http://dx.doi.org/10.1016/j.ajpath.2015.01.031)*

Ehlers-Danlos syndrome (EDS) is a hereditary connective tissue disorder characterized by joint hypermobility, skin extensibility, and connective tissue fragility.[1–5] The combined prevalence of all types of EDS is approximately 1 in 5000. More than half of these cases are characterized by joint hypermobility,[6] and hypermobility is one of the major diagnostic criteria for the classic subtype of EDS. Joint hypermobility can cause chronic joint and limb pain, recurring joint dislocation, and sports injuries with potential degenerative complications, including muscle weakness, precocious osteoarthritis, spondylosis, and lower bone mass.[6–9]

In more than 90% of patients with classic EDS, collagen V mutations have been identified,[3,10] and approximately half are null-allele mutations resulting in *COL5A1* haploinsufficiency.[10–12] Besides the null-allele mutations, mutations scattered throughout *COL5A1* and *COL5A2* genes and some mRNA splicing mutations in *COL5A1* also have been identified.[10] This finding has led to the proposal that classic EDS is a collagen V disease resulting from altered collagen V expression.[10]

Collagen V is a quantitatively minor, regulatory component in collagen I—rich connective tissues, including dermis, tendons and ligaments, bones, blood vessels, and cornea.[13] Collagen V content relative to collagen I varies from a high of 10% to 20% in cornea to 2% to 5% of the total fibril-forming collagens in most other tissues.[14,15] Collagen V regulates collagen fibrillogenesis by nucleating fibril assembly in *in vitro*

Supported by NIH/National Institute of Arthritis and Musculoskeletal and Skin Diseases grants AR044745 (D.E.B.) and AR065995 (L.J.S. and D.E.B.).

Disclosures: None declared.

http://dx.doi.org/10.1016/j.ajpath.2015.01.031

self-assembly assays, cell culture analyses, and mouse models.[14,16–19] The data support a model whereby the collagen V:I ratio in different tissues determines the initial diameter and number of fibrils assembled. By varying the number of collagen V nucleation sites for a given collagen I concentration, the fibroblast can regulate fibril number and diameter in a tissue-specific manner, ie, more sites result in increased fibrils assembled with smaller diameters.[13,17]

Several mouse models have been established to elucidate the function of collagen V tissue-specific fibril assembly. A traditional homozygous deletion in the *Col5a1* gene is embryonic lethal because of a virtual lack of fibril formation at the beginning of organogenesis in the early embryo, although the $Col5a1^{-/-}$ mice synthesize and secrete collagen I at a level comparable with that of wild-type controls.[18] This model demonstrates that collagen V is essential for the assembly of collagen I–containing fibrils in the low-collagen-concentration environment of the embryo and is consistent with a critical role in nucleation of fibril assembly. The heterozygous $Col5a1^{+/-}$ mice demonstrate haploinsufficiency, with approximately 50% of wild-type collagen V expression. $Col5a1^{+/-}$ mice are excellent models of classic EDS.[20] There were two subpopulations of fibrils in the mutant dermis. One had increased diameters and normal fibril structure, and these were immunoreactive for collagen V; the second group had very large diameters with aberrant fibril structure and were negative for collagen V reactivity. This suggests relatively normal assembly when nucleated with collagen, but the expression level of collagen V was insufficient to nucleate all available collagen I and, therefore, dysfunctional fibril assembly in the high-collagen-content environment. This abnormal fibril growth recapitulated that seen clinically in the dermis of EDS patients. In addition, the $Col5a1^{+/-}$ flexor digitorum longus tendon (FDL) also demonstrates decreased cross-sectional area and stiffness compared with that in the wild-type controls,[21] consistent with the joint hypermobility and dislocations seen in EDS patients.

To overcome the embryonic lethal phenotype and permit analyses of the roles of collagen V in the development and maturation of a tissue-specific extracellular matrix, our group created a conditional collagen V–null mouse model by using a *Cre/loxP* approach.[22] When targeted to the corneal stroma, a severe dysfunctional regulation of fibrillogenesis and corneal opacity was observed in the targeted collagen V–null mice. Unlike cornea, the tendon has a low collagen V content. The mature tendon contains uniaxial fibrils with a very heterogeneous population of fibril diameters, and the mechanical properties of the tendon depend on the increases in fibril diameter seen with development.[23]

Our aim was to explore specific regulatory roles for collagen V in tendons and ligaments, as well as its roles in the pathophysiology associated with joint hypermobility in classic EDS. Our conditional $Col5a1^{flox/flox}$ mouse model was targeted to tendons and ligaments using Cre driven by a Scleraxis (Scx) promoter (*Scx-Cre*) to produce the $Col5a1^{\Delta ten/\Delta ten}$ mouse model. *Scx-Cre* targets the deletion to tendons and ligaments. The data demonstrate that the absence of collagen V results in a disruption in tendon and ligament structure and function. In addition, there were consistent differences between the FDL tendon and the anterior cruciate ligament (ACL), indicating tissue-specific regulatory properties. The absence of collagen V also resulted in alterations in the joint consistent with the hypermobility seen in classic EDS.

Materials and Methods

Generation of Tendon- and Ligament-Specific $Col5a1^{\Delta ten/\Delta ten}$ Mice

Conditional $Col5a1^{flox/flox}$ mice were created by flanking exons 3 and 4 of the *Col5a1* gene with *loxP* elements and have been described previously.[22] *Scx-Cre* transgenic mice express Cre driven by the Scx promoter, thereby targeting expression to tendons and ligaments.[24] Tendon- and ligament- specific expression was characterized by breeding *Scx-Cre* mice with Cre reporter mTmG (membrane-Tomato/membrane-Green) mice (The Jackson Laboratory, Bar Harbor, ME). To generate tendon- and ligament-specific collagen V–null mice, we crossbred *Scx-Cre* transgenic mice with conditional $Col5a1^{flox/flox}$ mice for two generations to create $Scx\text{-}Cre^{+}/Col5a1^{flox/flox}$ ($Col5a1^{\Delta ten/\Delta ten}$) mice. The primers for the genotyping and characterization of $Col5a1^{\Delta ten/\Delta ten}$ mice were described previously.[22] All animal studies were performed in compliance with animal protocols approved by the Institutional Animal Care and Use Committee.

Immunoblotting

FDL tendons, ACL, skin, bone, and cornea were dissected from postnatal day (P)10 male mice. Protein extracts were prepared in 50 mmol/L Tris-HCl, pH 6.8, 1% SDS lysis buffer with proteinase inhibitors (Thermal Scientific, Waltham, MA). Protein lysates (20 μg) were separated on a 4% to 12% Bis-Tris gel (Life Technologies, Grand Island, NY) and transferred onto a Hybond-C membrane (GE Healthcare, Pittsburgh, PA). The membrane was hybridized with affinity purified anti-α1(V),[18] and anti-β-actin antibodies (Millipore, Billerica, MA). To analyze collagen V expression in FDLs and ACLs from wild-type C57BL/6 mice, we dissected control $Col5a1^{flox/flox}$ mice and $Col5a1^{\Delta ten/\Delta ten}$ mice, and the same procedures were followed.

Real-Time PCR

FDLs and ACLs were dissected from the mice at P10 and were cut into small pieces. Total RNA from FDL was extracted using the RNeasy Micro Kit (Qiagen, Germantown, MD). Total RNA (3 ng per well) was subjected to reverse transcription by using the High-Capacity cDNA Reverse Transcription Kit (Life Technologies), and real-time PCR was performed with SYBR Green PCR master

mix (Life Technologies) on a StepOnePlus Real-Time PCR System (Life Technologies). The primer sequences were as follows: *Col5a1*: forward, 5′-AAGCGTGGGAAACTGC-TCTCCTAT-3′, and reverse, 5′-AGCAGTTGTAGGTGA-CGTTCTGGT-3′; β-actin, forward, 5′-AGATGACCCAG-ATCATGTTTGAGA-3′, and reverse, 5′-CACAGCCTGGA-TGGCTACGT-3′. Each sample was run in triplicate, and data were analyzed using StepOne software version 2.0 (Life Technologies, Foster City, CA). β-Actin was used as an internal control to standardize the amount of sample total RNA.

Immunolocalization

FDL tendons were dissected from control $Col5a1^{flox/flox}$ mice and $Col5a1^{\Delta ten/\Delta ten}$ mice at P4 and P30 and were fixed in the fixative containing 4% paraformaldehyde, embedded in an OCT compound and frozen at −80°C. Cross sections (5 μm) were cut using an HM 505E cryostat (Thermo Fisher Scientific). For the ACLs, whole knee joints were removed from littermate control and knockout mice at P4, skinned, and trimmed of extra muscles. Sagittal sections (5 μm) containing longitudinal ACL were cut. Immunolocalization was performed using immunofluorescence microscopy to analyze expression of collagen V. Before the incubation with antibodies, the sections were pretreated with testicular hyaluronidase to enhance penetration. Anti-mouse collagen V antibody was used at 1:400. The secondary antibody was goat anti-rabbit IgG Alexa Fluor 568 (Life Technologies) at 1:400. Vectashield mounting solution with DAPI (Vector Laboratories, Burlingame, CA) was used as a nuclear marker. Images were captured using a CTR 5500 fluorescence microscope (Leica, Wetzlar, Germany) and DFC 340 FX digital camera (Leica). Antibody incubations and image acquisition were performed concurrently for sections of control $Col5a1^{flox/flox}$ and $Col5a1^{\Delta ten/\Delta ten}$ mice by using identical procedures and settings to facilitate comparison.

Gait Analysis

Footprints were recorded for gait analysis of individual mice. Hind limbs of the mouse were dipped in nontoxic paint, and the mouse was allowed to walk freely on a piece of white paper in a walkway consisting of two Plexiglas walls, spaced 8 cm apart. The footprint recording was repeated at least three times for each mouse. Parameters for stride length, intermediate toe spread, and total toe spread were calculated from walking tracks recorded on the paper. Stride length was the distance between adjacent prints made by the same hind limb.

Grip Strength

To assess musculoskeletal and motor function impairment of the conditional knockout mouse, we used a grip strength meter (San Diego Instruments, San Diego, CA) to record the peak force the animal exerted in grasping a grip placed at the forelimb. The grip strength meter was positioned horizontally, and the mouse was held by the tail and lowered toward the grip strength platform. The animal was allowed to grasp the forelimb grip with its forepaws. The mouse then was pulled steadily by the tail away from the rod until the mouse's grip was broken. The force applied to the grip just before the animal lost its grip was recorded as the peak tension. Ten measurements from each mouse were recorded, and the mean force was used to represent the grip strength for each mouse.

Biomechanics

Postnatal day 60 (P60) FDLs were analyzed as previously described[25] by using eight wild-type control mice and eight $Col5a1^{\Delta ten/\Delta ten}$ mice. Briefly, cross-sectional areas of the P60 tendons were measured using a custom laser-based device.[26] P60 tendons were clamped in custom test fixtures, and standard mechanical testing protocols were used as described. Student's *t*-tests were performed on cross-sectional area, stiffness, and elastic modulus comparing across genotype (significance at $P < 0.05$).

ACLs were analyzed using 19 control and 10 $Col5a1^{\Delta ten/\Delta ten}$ male mice at age P60. Briefly, hind limbs were obtained, and the ACL was dissected free of soft tissue, leaving only the tibia-ACL-femur complex intact, and Verhoeff stain was applied for optical strain tracking.[27] The femur and tibia were affixed in custom-built testing fixtures such that the femur was vertical and the tibia was at approximately 60 degrees of flexion. The ACL was tested using a standard testing protocol as described for the FDL but adjusted for a 1-mm gauge length for the ACL. Cross-sectional area was calculated assuming an ellipsoidal shape, with length and width measured in the coronal and sagittal planes. Local strain was measured optically, and parameters, ie, modulus and stiffness, were calculated using custom Matlab software version 2012a (Mathworks, Natick, MA). Modulus is the slope of the linear portion of the stress-versus-strain curve, where stress is the force divided by cross-sectional area and strain is the change in length divided by the initial length. Stiffness is a structural parameter that can vary with tissue size, but modulus is a property of the material. Maximum stress was calculated as maximum load divided by initial area. Comparisons were made between groups by using Student's *t*-tests with significance set at $P < 0.05$.

Transmission Electron Microscopy

FDLs and ACLs from $Col5a1^{\Delta ten/\Delta ten}$ and control $Col5a1^{flox/flox}$ mice at ages P4 and P30 were used for ultrastructural analysis. The samples were prepared for transmission electron microscopy as previously described.[25] Sections were examined and photographed at 80 kV by using a JEM-1400 transmission electron microscope (JEOL USA, Peabody, MA) and a Gatan Orius widefield side mount digital camera (Gatan, Warrendale, PA).

Fibril Diameter Measurement

Fibril diameter was analyzed as previously described.[21,28] Collagen fibril diameters in FDLs and ACLs from three different P30 mice from each genotype were analyzed. Four nonoverlapping cross-sectioned digital images were obtained at ×60,000 from the central areas of each specimen. Diameters were measured along the minor axis of cross sections by using an RM Biometrics-Bioquant Image Analysis System (Nashville, TN). Data analysis and histograms were created using Microsoft Excel 2007 (Redmond, WA). Fibril density was obtained as the fibril number per unit area.

Histologic Analysis

Col5a1$^{\Delta ten/\Delta ten}$ mice and *Col5a1*$^{flox/flox}$ control mice at P4 and P30 were whole-body perfused with 4% paraformaldehyde. Intact knee joints were dissected, decalcified, and embedded in paraffin. Sections (5 μm) were cut in the frontal plane toward the back or sagittal plane from lateral toward medial. Sections were collected from the central weight-bearing region of the tibial plateau on the basis of the presence of the ACL and anatomy of the lateral meniscus. Sections were stained with either H&E or Safranin O. Histologic images were captured using an Olympus BX61 TRF microscope and a DP72 12.8-megapixel digital color camera (Olympus, Center Valley, PA).

Results

Generation of a Tendon- and Ligament-Specific Conditional Collagen V—Null Mouse Model

To overcome the embryonic lethal phenotype in the traditional *Col5a1*-null mice,[18] a mouse line was established with *Col5a1* exons 3 and 4 flanked by *loxP* elements.[22] This conditional mouse line *Col5a1*$^{flox/flox}$ was crossed with a *Scx-Cre* mouse line. The *Scx-Cre* transgenic mouse line expresses Cre under the control of the regulatory sequence for the *Scx* gene that is expressed in tendon and ligament cells beginning with progenitor stages.[29,30] To determine the tissue specificity and efficacy of recombination driven by *Scx-Cre*, we crossed *Scx-Cre* mice with a Cre reporter (mTmG) mouse line.[31] The mTmG mouse is a dual-fluorescent Cre reporter mouse with *loxP* sites flanking a mT cassette. It expresses strong red fluorescence in all tissues including skin and tendon in the absence of *Cre* expression (Figure 1A). In contrast, when the mTmG mouse is crossed with an *Scx-Cre* mouse, the Cre recombinase in the tenocytes from the offspring excises the mT cassette and activates the downstream membrane-targeted enhanced green fluorescent protein (mG) cassette that expresses strong green fluorescence. The *Scx-Cre* recombinase activity is limited to tendons (Figure 1A) and ligaments (Figure 2A). The red fluorescence remained in other tissues, including skin, muscle, and bone tissues in the limb cross sections from P4 mice (Figure 1A).

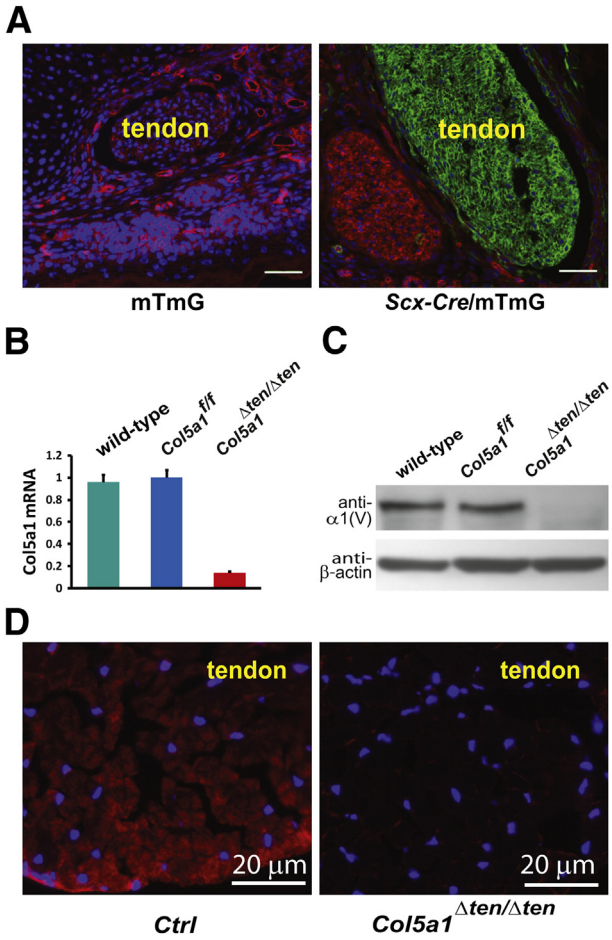

Figure 1 Targeted deletion of collagen V in flexor digitorum longus (FDL) tendons. **A:** Cre excision was targeted to tendons by using a Scleraxis promoter (*Scx-Cre*) in a double reporter (mTmG) mouse. Analysis of cross sections from postnatal day 4 (P4) limbs shows ubiquitous expression of red fluorescence (mT) in control mTmG mice. In contrast, *Scx-Cre*/mTmG mice show green fluorescence (mG) in the tendon, indicating targeted Cre excision. Other tissues show no Cre recombinase activity. DAPI (blue), nuclear localization. **B:** Col5a1 mRNA expression in the postnatal day 10 *Col5a1*$^{\Delta ten/\Delta ten}$ FDL is at background levels at real-time PCR. In contrast, expression in *Col5a1*$^{flox/flox}$ (*Col5a1*$^{f/f}$) control mice is comparable with that in the wild-type mice. **C:** Postnatal day 10 FDLs are collagen V null in *Col5a1*$^{\Delta ten/\Delta ten}$ mice. Immunoblot analysis using antibodies against the alpha 1 chain of collagen V [a1(V)] and against β-actin as a loading control. Control *Col5a1*$^{flox/flox}$ and wild-type mice express comparable collagen V. **D:** Collagen V immunoreactivity (red) is present in postnatal day 30 control (Ctrl) FDLs but absent in *Col5a1*$^{\Delta ten/\Delta ten}$ mice. DAPI (blue), nuclear localization. Scale bars = 20 μm (**A**).

These data are consistent with a lack of Cre excision in these tissues and demonstrate specific tendon and ligament targeting by using the *Scx-Cre* mouse.

To produce a targeted tendon and ligament collagen V—null mouse model, we bred *Scx-Cre* mice with the conditional *Col5a1*$^{flox/flox}$ mouse line[22] that produced *Scx-Cre*$^{+}$/*Col5a1*$^{flox/+}$ mice. Intercrossing *Scx-Cre*$^{+}$/*Col5a1*$^{flox/+}$ mice with *Col5a1*$^{flox/flox}$ mice generated mice homozygous for the floxed allele expressing Cre under the Scx promoter (*Scx-Cre*). The Cre excision of exons 3 and 4 resulted in mice with *Col5a1*-null tendons and ligaments (*Col5a1*$^{\Delta ten/\Delta ten}$). The expression of Col5a1 mRNA and collagen V was analyzed in

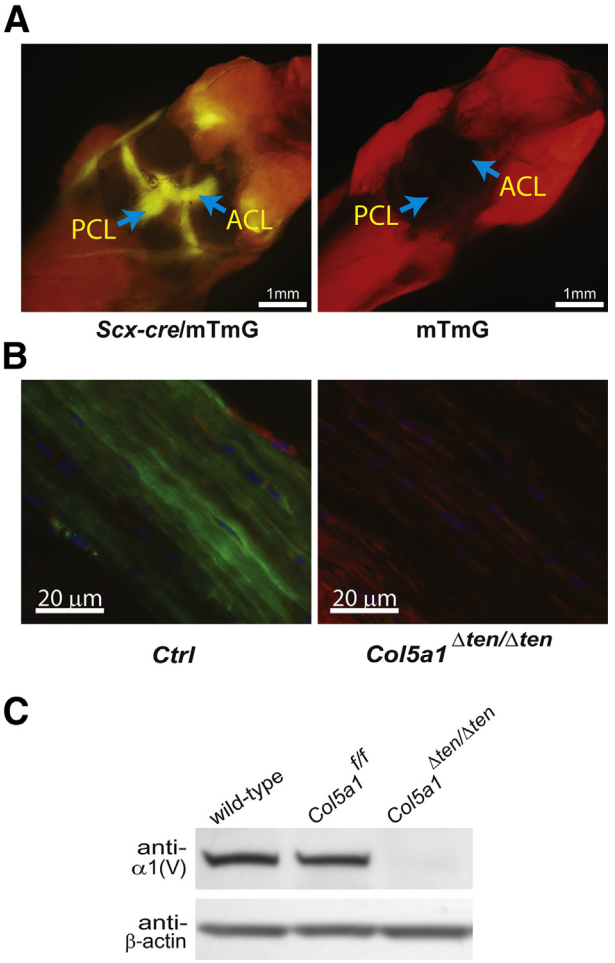

Figure 2 Targeted deletion of collagen V in anterior cruciate ligament (ACL) driven by Scleraxis-Cre (*Scx-Cre*). **A:** Posterior view of the knee joint of *Scx-Cre*/mTmG mouse at postnatal day 10 shows the ACL and posterior cruciate ligament (PCL) with green fluorescent protein expression (**left panel**). No green fluorescent protein is expressed in the mTmG control mouse knee joint (**right panel**). **Arrows** indicate the position of the ACL and PCL. The image was obtained with a fluorescence dissecting microscope. **B:** Immunofluorescence microscopy showed the depletion of collagen V expression in the $Col5a1^{\Delta ten/\Delta ten}$ ACL at postnatal day 10 (**right panel**) compared to the controls (**left panel**). Green, collagen V; red, phalloidin; blue, DAPI stained nucleus. **C:** Immunoblotting shows no expression of collagen V in $Col5a1^{\Delta ten/\Delta ten}$ ACLs. The $Col5a1^{flox/flox}$ ($Col5a1^{f/f}$) mouse ACL expressed the same amount of collagen V as did that of wild-type C57BL/6 mice. Ctrl, control; double reporter, mTmG.

the $Col5a1^{\Delta ten/\Delta ten}$ mice. In the P10 $Col5a1^{\Delta ten/\Delta ten}$ FDL tendons, Col5a1 mRNA expression was decreased to background levels compared with that in the wild-type P10 FDL tendons. Col5a1 mRNA expression in the control $Col5a1^{flox/flox}$ mouse FDL was comparable with that in wild-type FDL (Figure 1B). Consistent with the lack of mRNA expression, collagen V was completely absent in tendons from P10 $Col5a1^{\Delta ten/\Delta ten}$ mice, whereas the expression in the control $Col5a1^{flox/flox}$ FDL was comparable with that in wild-type mice (Figure 1C). In the P30 control mouse FDL tendon, collagen V was homogeneously distributed throughout the fiber bundles. In the $Col5a1^{\Delta ten/\Delta ten}$ FDL, the expression of collagen V was absent (Figure 1D). In addition, collagen V expression also was not detected in the ACLs of $Col5a1^{\Delta ten/\Delta ten}$ mice at immunofluorescence microscopy (Figure 2B), and this finding was confirmed by using immunoblot analysis (Figure 2C). These data indicate that the $Col5a1^{\Delta ten/\Delta ten}$ mouse is a tendon- and ligament-specific collagen V—null mouse model line.

Conditional Inactivation of Tendon and Ligament *Col5a1* Gene Expression Results in Abnormal Gait and Joint Phenotype

$Col5a1^{\Delta ten/\Delta ten}$ mice are viable; however, grossly they are easily distinguished from their Cre-negative littermates by the significantly smaller body size, slow movement, and abnormal gait in the young mice and joint dislocation in the older mice. We could speculate that the decreased body weight is the result of impaired mobility and function resulting in sedentary mice with difficulty feeding beginning at birth. In $Col5a1^{\Delta ten/\Delta ten}$ mice, the knee joints were positioned abnormally (Figure 3A). When the mouse was lifted gently by the tail, the two feet of the control mouse were positioned symmetrically, pointed to the front with the toes spread (Figure 3B). In contrast to the control mice, the feet of the $Col5a1^{\Delta ten/\Delta ten}$ mouse were not positioned symmetrically and usually were pointed outward or clutched together (Figure 3B). At age P60, the $Col5a1^{\Delta ten/\Delta ten}$ mouse was significantly smaller than the control mouse, and the body weight was 30% less than that of the control littermates (Figure 3C). Inside the cage, the $Col5a1^{\Delta ten/\Delta ten}$ mice tended to stay in one spot and were reluctant to move around. When walking freely on a piece of white paper in a walkway consisting of two Plexiglas walls, $Col5a1^{\Delta ten/\Delta ten}$ mice demonstrated major hindlimb differences in gait characteristics compared with that in $Col5a1^{flox/flox}$ mice. The $Col5a1^{\Delta ten/\Delta ten}$ mice dragged their hind limbs, with the body weight on the base of the foot. In contrast, the control mice placed their body weight on their toes and the middle part of the plantar surface. Compared with the mutant mice, the control mice had a consistently longer stride length and wider toe spread (Figure 3E). $Col5a1^{\Delta ten/\Delta ten}$ mice exhibited a less stable gait pattern than did $Col5a1^{flox/flox}$ mice.

To assess the musculoskeletal and motor function impairment of our mouse models, we measured the forelimb grip strength. The forelimb grip strength for the $Col5a1^{\Delta ten/\Delta ten}$ mice was significantly decreased compared with that of the control mice ($P < 0.001$) (Figure 3D). Because of the decreased grip strength, mutant mice could not hang on the cage wires only by their forelimbs. The $Col5a1^{\Delta ten/\Delta ten}$ mice also showed excessive joint laxity in the knee and ankle joints (Figure 3F). This increased joint laxity resembled the joint hypermobility seen in patients with classic EDS.[2,5] This phenotype progressed as the mice aged. The joint laxity led to instability, easy joint dislocation, and hypermobility. The majority of P90 and older $Col5a1^{\Delta ten/\Delta ten}$ mice had at least one joint dislocation in their four limbs. Both sexes of the $Col5a1^{\Delta ten/\Delta ten}$ mice were fertile. However, pups were produced and raised to weaning at a low rate; this may have been

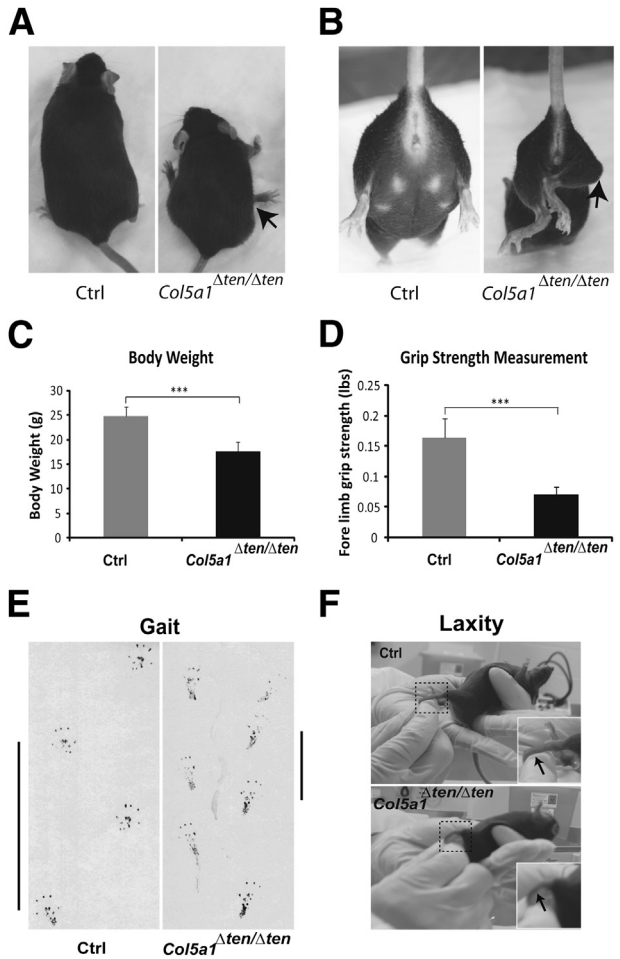

Figure 3 Joint laxity and aberrant gait in *Col5a1*$^{\Delta ten/\Delta ten}$ mice. **A** and **B:** *Col5a1*$^{\Delta ten/\Delta ten}$ mice with a targeted deletion of collagen V in tendons and ligaments show smaller size and deformation of the limbs in representative 8-month-old female mice (**arrows** indicate joint dislocation). **C:** Decreased body weight in *Col5a1*$^{\Delta ten/\Delta ten}$ mice. Postnatal day 60 male wild-type (n = 8) and mutant mice (n = 8) mice were used. **D:** Forelimb grip strength measurement from the same group of mice as in **C** show weakness of *Col5a1*$^{\Delta ten/\Delta ten}$ mice relative to control mice. **E:** Abnormal gait in *Col5a1*$^{\Delta ten/\Delta ten}$ mice. Representative hindlimb prints of control and *Col5a1*$^{\Delta ten/\Delta ten}$ mice. The control mice walk in a straight line with regular, even steps and wide toe spread. The *Col5a1*$^{\Delta ten/\Delta ten}$ mice show short stride lengths (**vertical bars**), with small toe spread. **F:** *Col5a1*$^{\Delta ten/\Delta ten}$ mice exhibit excess joint laxity compared with that in the control mice when the joint is overextended passively (**arrows**, ankle joint). ***$P < 0.001$. Ctrl, control.

due to the limited mobility in the adult *Col5a1*$^{\Delta ten/\Delta ten}$ mice (data not shown). These data indicate a severe impairment of tendon and ligament function in the absence of collagen V.

Early-Onset Osteoarthritis in *Col5a1*$^{\Delta ten/\Delta ten}$ Mice

The development of osteoarthritis was examined in control and *Col5a1*$^{\Delta ten/\Delta ten}$ mouse knee joints. Safranin O stains glycosaminoglycans in cartilage and is used for grading the development of osteoarthritis.[32] In the 1-month-old control mice, the articular cartilage of the medial and lateral tibial plateau or the medial and lateral femoral condyle had a smooth surface, evenly stained with Safranin O (Figure 4A). In the superficial zone of the articular cartilage, one or two layers of flat cells were arranged tangentially, and round cells were observed in the middle zone above the tidemark. In contrast, the *Col5a1*$^{\Delta ten/\Delta ten}$ mouse knees showed uneven staining with Safranin O in weight-bearing cartilage regions, with formation of fibrillations and further degeneration demonstrated by the presence of an osteophyte in severe cases (Figure 4B). These data demonstrate osteoarthritic progression as an indirect outcome of joint hypermobility as a result of collagen V deficiency in tendons and ligaments stabilizing the joint.

Altered Biomechanical Properties of FDLs in *Col5a1*$^{\Delta ten/\Delta ten}$ Mice

Cross-sectional area, stiffness, and modulus were analyzed (Figure 5). Cross-sectional area showed a significant

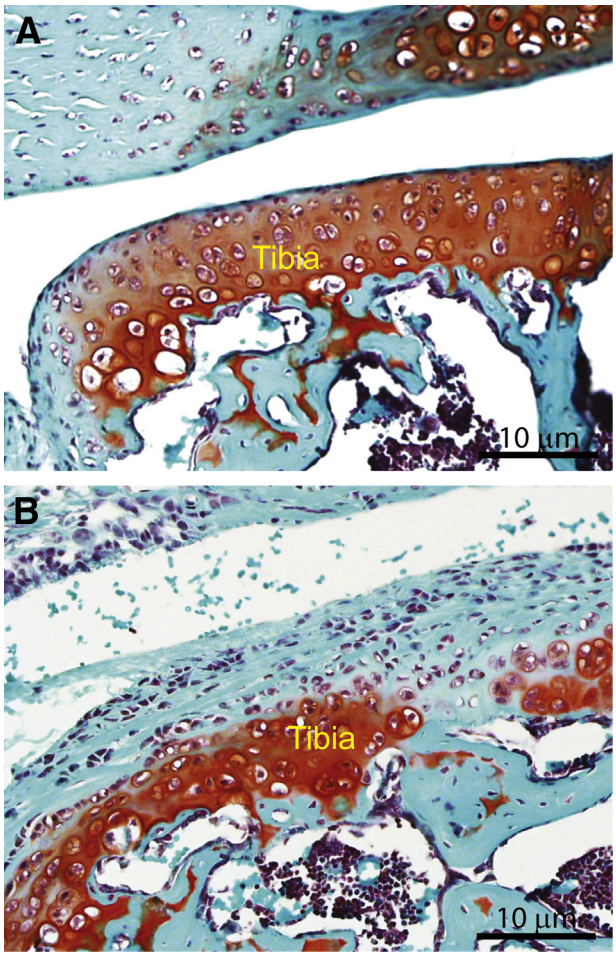

Figure 4 Early-onset osteoarthritis in *Col5a1*$^{\Delta ten/\Delta ten}$ mice. Representative histologic sections of tibial condyles in control and *Col5a1*$^{\Delta ten/\Delta ten}$ mice at postnatal day 30. Decalcified knee joint embedded in OCT. Frontal sections of the knee joint were stained with Safranin O and Fast green. **A:** The cartilage surface in the control mouse is smooth. **B:** The lateral surface of the tibia condyles in *Col5a1*$^{\Delta ten/\Delta ten}$ knee joint is covered with fibrous tissue and chronic inflammation cells. The cartilage erosion, chondrocyte death, and proteoglycan depletion indicate the onset of osteoarthritis in *Col5a1*$^{\Delta ten/\Delta ten}$ knee joint.

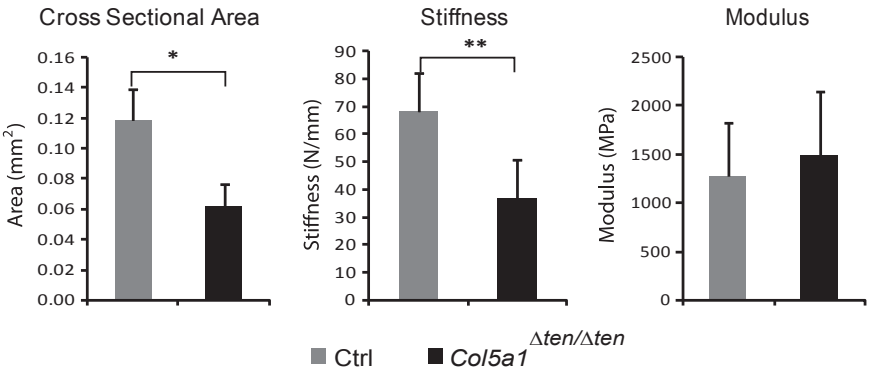

Figure 5 Altered biomechanical properties in *Col5a1*$^{\Delta ten/\Delta ten}$ flexor digitorum longus. Cross-sectional area, stiffness, and modulus were measured in postnatal day 60 (P60) male flexor digitorum longus tendons from *Col5a1*$^{\Delta ten/\Delta ten}$ and *Scx-Cre* control mice. The significant decrease in cross-sectional area and stiffness in *Col5a1*$^{\Delta ten/\Delta ten}$ FDLs is consistent with the joint laxity phenotype. The modulus is comparable in both genotypes. *$P < 0.05$, **$P < 0.01$.

difference between the control and mutant mice, with the latter being significantly smaller ($P < 0.01$). This is consistent with significant difference in body weight in these two groups of mice. Stiffness also showed a significant difference between the two genotypes, with the *Col5a1*$^{\Delta ten/\Delta ten}$ tendons being less stiff ($P < 0.05$). However, there were no significant differences detected in modulus between the groups ($P = 0.24$). These results indicate that the tendons of *Col5a1*$^{\Delta ten/\Delta ten}$ mice were smaller and, thus, were less stiff. The decreased stiffness is consistent with a role in joint laxity in EDS.

Aberrant Fiber Structure and Organization in Collagen V—Null FDL Tendons

The regulatory roles of collagen V in the assembly of fiber structure, ie, organization of fibrils into fibers associated with tendon fibroblasts, was analyzed at P4 during an early stage of tendon development. In the wild-type mouse FDL, fibers were organized uniaxially throughout the tendon. The fibers were relatively uniform in size and were defined by tenocyte cytoplasmic processes that defined microdomains where fibrils were organized into fibers. Collagen protofibrils can be seen in the cytoplasmic processes during deposition (Figure 6, A and B). In contrast, the *Col5a1*$^{\Delta ten/\Delta ten}$ tendon demonstrated less-organized fibers. Fibril organization into fibers also was disrupted, with fewer, larger fibers that were less organized than in the wild-type controls. The fibers were packed less regularly, with more and irregular spaces separating them. In addition, the tenocyte processes defining the microdomains were less organized than in the controls and were associated with the disruption in fiber organization (Figure 6, C and D).

Fibril assembly also was altered in the *Col5a1*$^{\Delta ten/\Delta ten}$ compared with in the wild-type FDL. Fibril diameters were more heterogeneous in P30 *Col5a1*$^{\Delta ten/\Delta ten}$ FDLs than in the wild-type tendons (Figure 7, A and B). In addition, the mutant fibrils often demonstrated irregular cross-sectional profiles compared with the circular profiles seen in control mice. Analyses of the diameter distributions demonstrated a broader distribution with a right-hand shoulder representing larger-diameter fibrils in the *Col5a1*$^{\Delta ten/\Delta ten}$ than in the control FDLs (Figure 7C). In addition, a broadening of the diameter distribution was observed as an increase in the median from 119 nm in the control mouse FDL to 129 nm in the *Col5a1*$^{\Delta ten/\Delta ten}$ FDL; the interquartile range Q4 to Q3 increased from 82 to 117 nm, and the interquartile range Q3 to Q1 increased from 139 to 168 nm. The fibril diameter (means ± SD) was significantly increased from 114 ± 47 nm in the control mouse FDL to 131 ± 64 nm in the *Col5a1*$^{\Delta ten/\Delta ten}$ FDL (Figure 7D). The number of fibrils decreased, with fibril density approximately 30% less than in control FDLs (Figure 7E). The assembly of fewer and

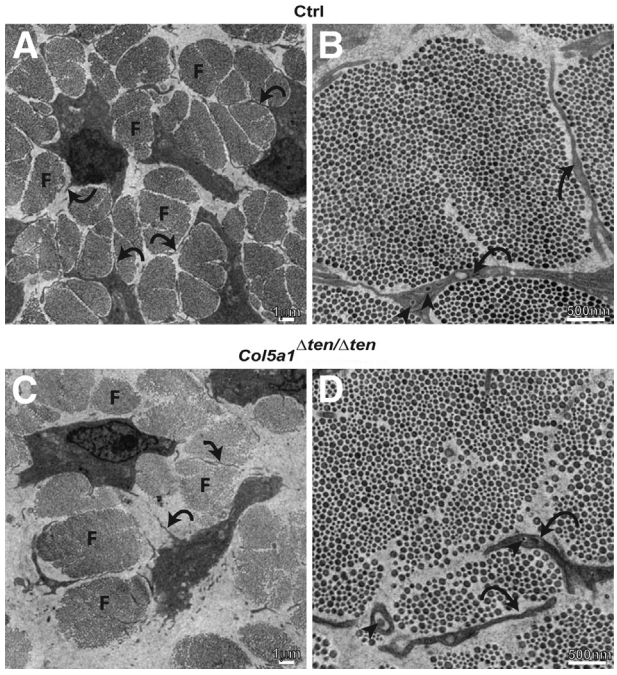

Figure 6 Aberrant fiber structure and organization in *Col5a1*$^{\Delta ten/\Delta ten}$ tendons during early tendon development. **A** and **B:** Postnatal day 4 control (Ctrl) mouse flexor digitorum longus (FDL) contained organized fibers (F) that are relatively uniform in size. The fibers were present in microdomains that were defined by tenocyte cytoplasmic processes (**curved arrows**). **B** and **D:** Collagen protofibrils can be seen during deposition (**arrowhead**). **C** and **D:** *Col5a1*$^{\Delta ten/\Delta ten}$ mouse FDLs have less-organized fibers (F). In *Col5a1*$^{\Delta ten/\Delta ten}$ FDLs, there are fewer fibers than in the wild-type controls. The collagen V—null FDLs have larger fibers with more heterogeneity in size than in control tendons. In addition, in the absence of collagen V, the fibers are less organized, ie, less regularly packed, with more space separating them than in the controls. In addition, the tenocyte processes (**curved arrows**) defining the microdomains are less organized than in the controls.

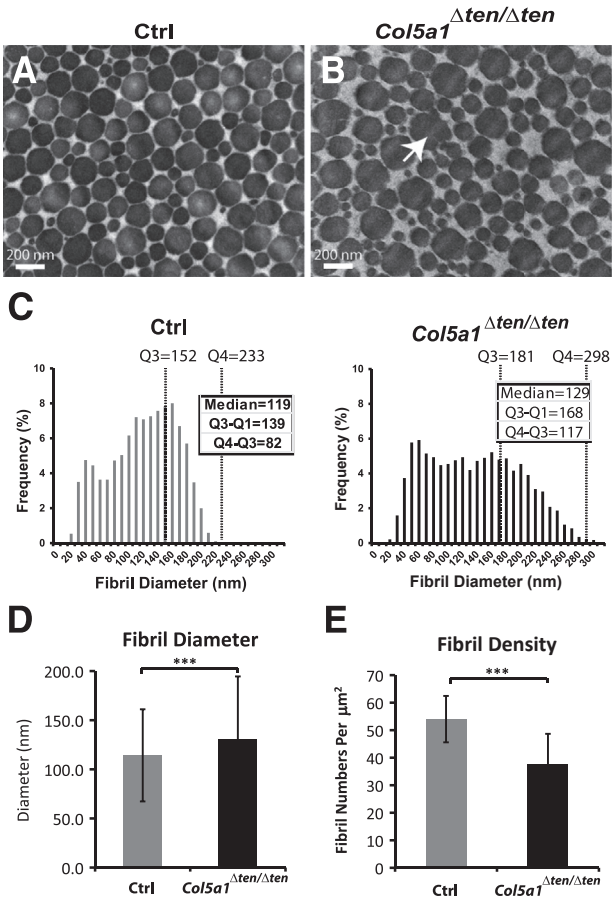

Figure 7 Abnormal fibril structure in mature *Col5a1*$^{\Delta ten/\Delta ten}$ tendons. **A** and **B:** The *Col5a1*$^{\Delta ten/\Delta ten}$ flexor digitorum longus (FDL) has larger and more heterogeneous fibrils than do the wild-type controls. In addition, fibrils assembled in collagen V—null tendons show aberrant structures (**arrow**). **C:** Histograms represent the distribution of fibril diameters in the FDL tendon of control and *Col5a1*$^{\Delta ten/\Delta ten}$ mice. The *Col5a1*$^{\Delta ten/\Delta ten}$ mice have broader distribution of the fibril diameters, with increased fibril numbers of both small-diameter and large-diameter fibrils. The diameter was measured in three different mice of each group, with seven images from each mouse. **D:** The mean fibril diameter is increased significantly in the FDL of *Col5a1*$^{\Delta ten/\Delta ten}$ mice. **E:** The fibril density is decreased significantly in the FDL of *Col5a1*$^{\Delta ten/\Delta ten}$ mice. The means ± SD, $n = 21$, and Student's *t*-test (**D** and **E**). All FDLs were from male mice at postnatal day 30. ***$P < 0.001$. Ctrl, control; Q, quartile.

larger-diameter fibrils is consistent with dysregulated fibril nucleation and assembly in the absence of collagen V.[21]

Joint laxity and dislocation are the major gross phenotypes in the *Col5a1*$^{\Delta ten/\Delta ten}$ mice, consistent with a classic EDS joint phenotype. The structural and functional data from the FDL are consistent with a role in joint stability. Data derived from one tendon or ligament often is generalized to tendons and ligaments, but this flexor tendon does not function directly to stabilize joints *in vivo*. Therefore, a ligament intrinsic to the joint, the ACL, which is a critical ligament in maintaining knee stability, was analyzed.

Expression of Collagen V Is Higher in ACL than in FDL

Collagen V was analyzed in ACL, FDL, and other connective tissues in wild-type mice at P10. Consistent with other results from reports, collagen V expression in FDL was very low and in cornea was very abundant, accounting for 10% to 20% of total collagen.[14] Collagen V expression in ACL was substantially higher than that in the FDL; ACL expression was comparable with or higher than that in skin and bone but lower than that in cornea (Figure 8). Col5a1 mRNA expression in P10 mice also indicated higher Col5a1 mRNA expression in the ACL relative to that in the FDL (data not shown). These data suggested that the different collagen V expression levels in ACL versus FDL may contribute to tissue-specific structure and function in tendons and ligaments.

Altered ACL Fibrillogenesis in *Col5a1*$^{\Delta ten/\Delta ten}$ Mice

The ACL showed a severe disruption of fibrillogenesis in *Col5a1*$^{\Delta ten/\Delta ten}$ mice relative to the control mice at age P30 (Figure 9, A and B). Unlike in FDL tendon, the fibril bundles in ACL are not aligned in parallel, especially at the distal and proximal ends. However, the fibril arrangement is in parallel to the axis, and fibril cross sections were compared only in the ACL midsubstance. At P30, the fibril diameter distribution patterns were similar in the control ACLs and FDLs. The fibril diameters were heterogeneous, with larger and smaller diameter fibrils interspersed (Figure 9A). However, the fibril diameters in ACLs were smaller than in FDLs of comparable age. Diameters (means ± SD) were 67 ± 27 nm in the ACL (Figure 9D) compared with 118 ± 47 nm in the FDL (Figure 7D) at age P30. Compared with those in control mice, *Col5a1*$^{\Delta ten/\Delta ten}$ ACLs had a broader fibril diameter distribution (Figure 9C). The fibril diameter distribution showed a significant shift to the larger fibrils in *Col5a1*$^{\Delta ten/\Delta ten}$ mice, with a reduction in small-diameter fibrils in ACLs from *Col5a1*$^{\Delta ten/\Delta ten}$ mice. The median diameter of the fibrils was 104 nm, ranging from 23 to 256 nm, and the interquartile range Q4 to Q3 was 119 nm. In contrast, the median fibril diameter for the control mice was 64 nm, ranging from 13 to 151 nm, and the interquartile range Q4 to Q3 was 63 nm (Figure 9C). A statistical analysis demonstrated a significant increase in the mean fibril diameter ($P < 0.001$) in the ACL of *Col5a1*$^{\Delta ten/\Delta ten}$ mice compared with that in control mice (Figure 9D). In addition, the number of fibrils assembled in the *Col5a1*$^{\Delta ten/\Delta ten}$ ACLs was reduced compared with that in controls, with a significant decrease in fibril density ($P < 0.001$) (Figure 9E). The decrease in density was associated with an increase in fibril diameter, as well as an increase in interfibril spacing. These data indicated that collagen V is required for normal fibrillogenesis in the ACL ligament.

Severe Reduction in the Biomechanical Properties of Collagen V—Null ACL

During tissue preparation and biomechanical testing, the ACLs from *Col5a1*$^{\Delta ten/\Delta ten}$ mice were very fragile. ACLs frequently were broken before dissecting, and even very small

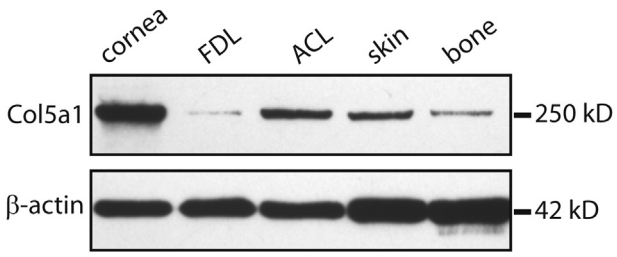

Figure 8 High collagen V content in anterior cruciate ligament (ACL) versus flexor digitorum longus (FDL). Immunoblot analysis shows different collagen V expression levels in different tissues of postnatal day 30 wild-type C57BL/6 mice. Cornea expresses the most collagen V, followed by ACL, which is comparable with that in the skin but much higher than that in FDL and bone. β-Actin was used as the protein loading control.

loads during careful preparation of the ACLs for testing caused some ligaments to fail. This occurred only in the *Col5a1*$^{\Delta ten/\Delta ten}$ mice and not in the control mice. The *Col5a1*$^{\Delta ten/\Delta ten}$ ACLs demonstrated a significantly lower maximum load and maximum stress compared with that in wild-type controls (data not shown). In contrast to the FDL, there was no significant difference in cross-sectional area between *Col5a1*$^{\Delta ten/\Delta ten}$ and wild-type ACLs. However, the *Col5a1*$^{\Delta ten/\Delta ten}$ ACLs had a significantly lower stiffness and modulus compared with those in the controls ($P < 0.001$) (Figure 10). In the absence of a change in cross-sectional area, results support a change in the material properties of the ACL in the absence of collagen V. The mechanical changes in the ACL were much more dramatic than the changes in the FDL, suggesting that collagen V has a greater role in the ACL.

Disruption of Higher-Order Structure in ACLs from *Col5a1*$^{\Delta ten/\Delta ten}$ Mice

In wild-type ACLs, running from the anterior intercondylar region of the proximal tibia to the medial aspect of the lateral femoral condyle within the intercondylar groove, well-organized fibril bundles and fibroblasts were aligned parallel to the stress axis in the ACL midsubstance (Figure 11A). In contrast, in the knees from *Col5a1*$^{\Delta ten/\Delta ten}$ mice, the orientation of ACL fibril bundles was disorganized and wavy. Patchy infiltration of lymphocytes and increased vasculature also were present around the knee joint, consistent with soft-tissue inflammation, suggesting a secondary defect resulting from ligament injury in the unstable joint (Figure 11A). Collagen fiber organization in the ACL was analyzed using picrosirius red staining with polarized light microscopy (Figure 11B). Large bright, orange-red collagen fibers were arranged in parallel and were well organized in control mouse ACL. In contrast, small and wavy collagen fibers were sparse and disorganized in *Col5a1*$^{\Delta ten/\Delta ten}$ mouse ACL, indicating that collagen fibers were smaller and less organized. In the *Col5a1*$^{\Delta ten/\Delta ten}$ ACL, it is noteworthy that there was a consistent difference in crimping when compared with that in the controls (Figure 11B), which would be consistent with increased elasticity and joint hypermobility.

Discussion

The targeted deletion of collagen V in tendons and ligaments created a mouse model (*Col5a1*$^{\Delta ten/\Delta ten}$) that faithfully recapitulates the joint laxity seen clinically in patients with classic EDS. The joint phenotype is the result of structural and functional changes in tendons and ligaments, especially the ACL, that is essential for the stabilization of the lower limb joint. Tendons and ligaments are multiunit hierarchical structures that contain collagen molecules, collagen fibrils, collagen fibers, and fascicles organized parallel to the geometric axis.[33–35] Collagen I accounts for the majority of the collagen mass, whereas collagen V forms heterotypic fibrils with collagen I in the matrix of different tissues to regulate the fibril nucleation and initiation of fibrillogenesis.[18,21,36] The *Col5a1*$^{-/-}$ mouse model was embryonic lethal because of a virtual lack of fibril

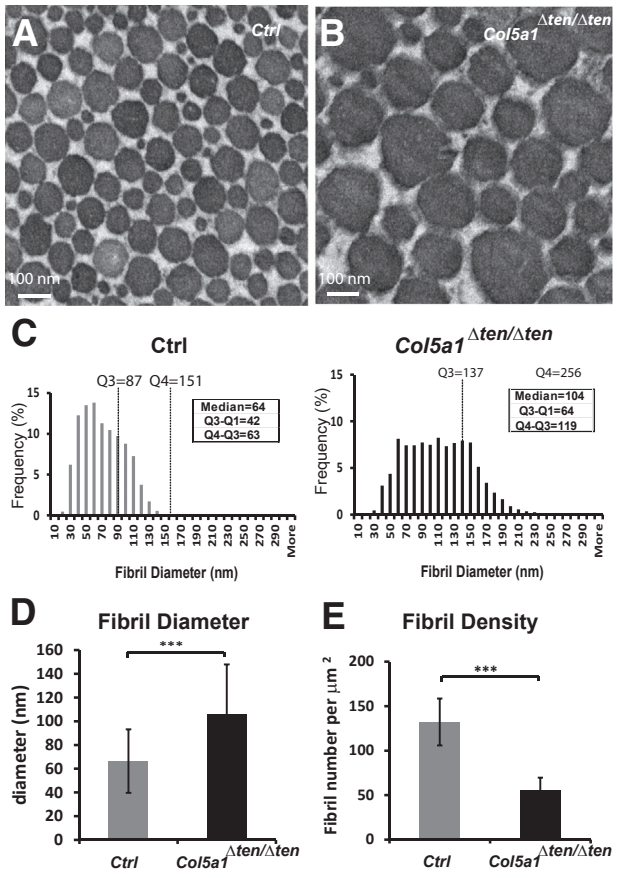

Figure 9 Abnormal anterior cruciate ligament (ACL) structure in the *Col5a1*$^{\Delta ten/\Delta ten}$ mouse. **A** and **B:** Transmission electron microscopy shows a significant increase in fibril diameter and aberrant fibril structure in the *Col5a1*$^{\Delta ten/\Delta ten}$ ACL. The alterations in the collagen V–null ACL were more severe. **C:** Histograms show the broader distribution of fibril diameters in the ACL of *Col5a1*$^{\Delta ten/\Delta ten}$ mice compared with that in the control mice. **D:** The mean fibril diameter is increased significantly in the ACL of *Col5a1*$^{\Delta ten/\Delta ten}$ mice ACL. **E:** The fibril density was decreased significantly in *Col5a1*$^{\Delta ten/\Delta ten}$ mice. Fibril diameter and density were measured in three different mice of each group, with three to seven images from each mouse; the data are presented as means ± SD, and Student's *t*-test was used (**C**–**E**). All mice were postnatal day 30 males. ***$P < 0.001$. Ctrl, control; Q, quartile.

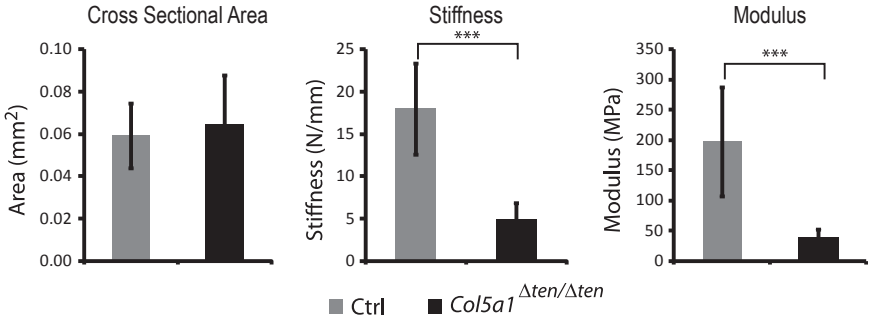

Figure 10 Altered biomechanical properties in anterior cruciate ligament (ACL) of *Col5a1*$^{\Delta ten/\Delta ten}$ mice. The biomechanical properties are altered significantly in the absence of collagen V, with a significant decrease in stiffness and modulus in the *Col5a1*$^{\Delta ten/\Delta ten}$ ACL compared with that in the controls (Ctrl). ***$P < 0.001$.

formation. However, the *Col5a1*$^{\Delta ten/\Delta ten}$ mice are viable and fertile. The severe disruption in tendon and ligament structure and function results in sedentary mice with impaired mobility. However, unlike in the *Col5a1*$^{-/-}$ mouse model, the tendons and ligaments of the *Col5a1*$^{\Delta ten/\Delta ten}$ mice assembled fibrils. The embryo 10.5 days post coitum has a low-collagen-concentration environment, and the presence of collagen V as a nucleator to lower the critical concentration required for initiation of fibril assembly is essential. In contrast, developing tendons have a high-collagen-concentration environment in which fibril assembly can occur in the absence of collagen V, as is observed with *in vitro* self-assembly assays.[17] However, the regulation conferred by heterotypic collagen I/V interactions is absent, resulting in the dysfunctional fibril and matrix assembly observed.

Altered Fibrillogenesis in Collagen V Mouse Models

Previous work in a *Col5a1*$^{+/-}$ haploinsufficient mouse model demonstrated increased fibril diameters and a subpopulation of fibrils that were large and structurally aberrant in the dermis, consistent with the classic EDS skin phenotype.[20] However, tendon structure in the haploinsufficient mouse model did not show major structural changes.[21] In contrast, the *Col5a1*$^{\Delta ten/\Delta ten}$ mouse model demonstrates major changes in tendon and ligament fibril structure, including an increase in fibril diameter and decrease in fibril density. This structural change is consistent with the fibril changes in EDS patients.[37] This suggests that collagen V must be present above a specific concentration for assembly of normal fibrils, but higher concentrations are required for structural and functional integrity of the tendon.

Altered Fiber Structure and Organization in Collagen V—Null Mice

In addition to the changes in the fibril formation, collagen fiber organization also is altered in the *Col5a1*$^{\Delta ten/\Delta ten}$ tendon. *Col5a1*$^{\Delta ten/\Delta ten}$ FDLs have less-organized tenocytes, resulting in fewer and larger fibers that are disorganized compared with those in the wild-type controls. This finding suggests that the loss of collagen V may alter cell—extracellular matrix interactions. Tendon fibroblasts establish a hierarchy of extracellular compartments associated with assembly of fibrils, fibril bundles, and fibers during development.[23,38,39] This hierarchy of microdomains allows control over the extracellular events in matrix assembly. Results from a recent study indicate that collagen V is localized preferentially on the tenocyte surface as distinct foci in tendons and in cell culture. This indicates that collagen V associates with the tenocyte surface, where it is proposed to function in regulation of collagen assembly and cell-directed fibril deposition.[40] Collagen V also is present in a pericellular—cell-associated matrix extract from developing tenocytes.[41] Collagen V binds to extracellular matrix proteins such as collagens, enzymes, and growth factors through the α1-N-propeptide and is involved in extracellular matrix homeostasis and bridging function in the cell-matrix environment.[42] Depletion of collagen V in tendon may destroy the binding of extracellular matrix proteins to the cells and further affect the tenocyte-directed fibril deposition, fiber formation, and higher-level hierarchical organization. However, the detailed mechanism is still unclear and requires further investigation.

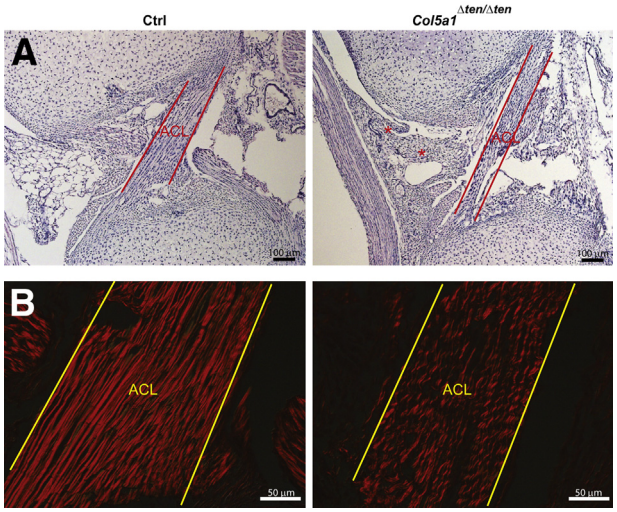

Figure 11 Targeted depletion of collagen V in tendon and ligament induces joint instability. **A:** Joint laxity and chronic fibrous inflammation presented in *Col5a1*$^{\Delta ten/\Delta ten}$ mice knee joints at postnatal day 4. Sagittal sections of knee joints from postnatal day 4 mice show that the fibroblasts and fibers of the anterior cruciate ligament (ACL) align parallel in the ACL midsubstance in the control (Ctrl) mice. In the *Col5a1*$^{\Delta ten/\Delta ten}$ ACL, the fibers were disorganized and wavy. The **asterisks** show synovial inflammation that contained fibrous connective tissue, blood vessels, and chronic inflammatory cells in the *Col5a1*$^{\Delta ten/\Delta ten}$ ACL. Stain: H&E. **B:** Polarized light microscopy in control mice shows large, well-organized ACL fibers. In contrast, the fibers in *Col5a1*$^{\Delta ten/\Delta ten}$ ACL are wavy and smaller. The specimens were the same as in **A**. Stain: picrosirius red.

Altered Biomechanical Properties in *Col5a1*$^{\Delta ten/\Delta ten}$ Mice

Biomechanical studies of the *Col5a1*$^{+/-}$ haploinsufficient[20] and *Col5a1*$^{\Delta ten/\Delta ten}$ FDLs demonstrate decreased cross-sectional area and stiffness. However, the modulus does not change significantly. From a mechanical perspective, this finding suggests that the material is functionally the same between groups, with differences primarily due to the size of the tissue. The changes in FDLs are relatively mild when compared with the severe biomechanical phenotype of the *Col5a1*$^{\Delta ten/\Delta ten}$ ACL, with a change in stiffness and modulus but no change in cross-sectional area compared with those in the controls. Unlike the FDL data, these data suggest a change in the material properties of the ACL because of the alterations in the structural organization. The FDL tendon is neither a weight-bearing tendon nor a direct joint-stabilizing tendon. Conversely, the ACL is intrinsic to the joint and essential for its stabilization, as well as one of the most vulnerable tendons or ligaments in the body.[43] The differences in mechanical and structural properties in the FDL and ACL suggest that collagen V is a critical regulator of tendon- and ligament-specific properties. To our surprise, compared with collagen V expression in the FDL, collagen V expression is substantially higher in the ACL. The collagen V level in ACL was comparable with or slightly higher than that in skin and substantially higher than that in FDL and bone, although it is still lower than that in cornea. This is the first time that the collagen V expression level in ACL has been reported. It is possible that the higher collagen V expression in the ACL confers tissue-specific regulatory properties. The resulting ACL-specific fibrillogenesis would yield a matrix structure with a primary function in joint stabilization.

Mouse Model for Classic EDS

When collagen V is knocked out in *Col5a1*$^{\Delta ten/\Delta ten}$ tendons and ligaments, there is a significant increase in fibril diameter and decrease in fibril density. The alterations in collagen organization and structure influence the biomechanical properties. A similar disorganization and dysfunction is found in the tendons of classic EDS patients bearing a *COL5A1* mutation.[37] The smaller tendon, reduced stiffness, and modulus are consistent with a hypermobile joint phenotype supported by the loose joint capsule, changes in gait, and changes in walking patterns. *Col5a1*$^{\Delta ten/\Delta ten}$ ligaments are easy to rupture. This finding, coupled with joint laxity and dislocation, could lead to early-onset osteoarthritis as a secondary effect to joint hypermobility, as was observed in the *Col5a1*$^{\Delta ten/\Delta ten}$ mouse model. The joint hypermobility phenotype progressed dramatically with age. The phenotype in the *Col5a1*$^{\Delta ten/\Delta ten}$ is more severe than in EDS patients because *Col5a1*$^{\Delta ten/\Delta ten}$ tendons and ligaments are null for collagen V, whereas most EDS patients harbor *COL5A1* mutations in only one allele. However, the mouse provides a valid model that faithfully recapitulates the clinical joint phenotype. Male mice were used in this initial study to ensure that the studies were controlled appropriately so that phenotypic differences would be explained only by gene dosage effects. In future work, it would be of interest to analyze potential sex differences in the mouse model to address the fact that female patients present more with classic EDS than do male patients.

Conclusions

Our results indicate that collagen V plays a critical regulatory role in the fibrillogenesis of tendons and ligaments. The deficiency of collagen V targeted to tendons and ligaments impairs normal FDL and ACL function, with differential tissue-specific effects. The absence of collagen V results in altered structure and functional properties, resulting in a severe joint hypermobility phenotype analogous to that observed in EDS patients. This mouse model provides, for the first time, the ability to target collagen V specifically in the musculoskeletal system, resulting in a severe joint phenotype that faithfully recapitulates the clinical phenotype observed in classic EDS patients. Therefore, an animal model of joint laxity has been created, providing a critical tool for the development of therapeutic interventions for EDS patients, as well as a larger group of non-EDS patients with joint laxity. Model availability provides a unique opportunity to evaluate a host of potential therapeutic agents, such as matrix metalloproteinase inhibitors like doxycycline,[44,45] or agents that have been tried in attempts to control metastatic cancer but failed because of patients developing the complication of dose-dependent, reversible joint stiffness.[46,47] In summary, the *Col5a1*$^{\Delta ten/\Delta ten}$ mouse model is a model for the EDS and hypermobile joint phenotype and can be used in future preclinical studies of injury, as well as clinical interventions for treatment of EDS and patients with hypermobile joints.

Acknowledgments

We thank Drs. Michael Mienaltowski (University of California Davis) and Patricia Teran-Yengle (University of South Florida) for helpful discussions and Qingmei Yao (University of South Florida) for the expert technical assistance with the maintenance of the mouse lines.

References

1. Beighton P, De Paepe A, Steinmann B, Tsipouras P, Wenstrup RJ: Ehlers-Danlos syndromes: revised nosology, Villefranche, 1997. Ehlers- Danlos National Foundation (USA) and Ehlers-Danlos Support Group (UK). Am J Med Genet 1998, 77:31–37
2. De Paepe A, Malfait F: The Ehlers-Danlos syndrome, a disorder with many faces. Clin Genet 2012, 82:1–11
3. Malfait F, De Paepe A: The Ehlers-Danlos syndrome. Adv Exp Med Biol 2014, 802:129–143
4. Malfait F, Wenstrup RJ, De Paepe A: Clinical and genetic aspects of Ehlers-Danlos syndrome, classic type. Genet Med 2010, 12:597–605
5. Steinmann B, Royce PM, Superti-Furga A: The Ehlers-Danlos syndrome. Edited by Royce PM, Steinmann B. Connective Tissue and Its

Heritable Disorders: Molecular, Genetic, and Medical Aspects. ed 2 New York, Wiley-Liss, 2002, pp 431–523
6. Castori M: Ehlers-danlos syndrome, hypermobility type: an underdiagnosed hereditary connective tissue disorder with mucocutaneous, articular, and systemic manifestations. ISRN Dermatol 2012, 2012: 751–768
7. Beighton P, Horan F: Orthopaedic aspects of the Ehlers-Danlos syndrome. J Bone Joint Surg Br 1969, 51:444–453
8. Stanitski DF, Nadjarian R, Stanitski CL, Bawle E, Tsipouras P: Orthopaedic manifestations of Ehlers-Danlos syndrome. Clin Orthop Relat Res 2000:213–221
9. Ainsworth SR, Aulicino PL: A survey of patients with Ehlers-Danlos syndrome. Clin Orthop Relat Res 1993:250–256
10. Symoens S, Syx D, Malfait F, Callewaert B, De Backer J, Vanakker O, Coucke P, De Paepe A: Comprehensive molecular analysis demonstrates type V collagen mutations in over 90% of patients with classic EDS and allows to refine diagnostic criteria. Hum Mutat 2012, 33:1485–1493
11. Malfait F, Coucke P, Symoens S, Loeys B, Nuytinck L, De Paepe A: The molecular basis of classic Ehlers-Danlos syndrome: a comprehensive study of biochemical and molecular findings in 48 unrelated patients. Hum Mutat 2005, 25:28–37
12. Malfait F, De Paepe A: Molecular genetics in classic Ehlers-Danlos syndrome. Am J Med Genet C Semin Med Genet 2005, 139C:17–23
13. Birk DE, Bruckner P: Collagens, suprastructures and collagen fibril assembly. Edited by Mecham RP. In The Extracellular Matrix: an Overview, Vol 1. New York, Springer, 2011, pp 77–115
14. Birk DE: Type V collagen: heterotypic type I/V collagen interactions in the regulation of fibril assembly. Micron 2001, 32:223–237
15. Segev F, Héon E, Cole WG, Wenstrup RJ, Young F, Slomovic AR, Rootman DS, Whitaker-Menezes D, Chervoneva I, Birk DE: Structural abnormalities of the cornea and lid resulting from collagen V mutations. Invest Ophthalmol Vis Sci 2006, 47:565–573
16. Marchant JK, Hahn RA, Linsenmayer TF, Birk DE: Reduction of type V collagen using a dominant-negative strategy alters the regulation of fibrillogenesis and results in the loss of corneal-specific fibril morphology. J Cell Biol 1996, 135:1415–1426
17. Birk DE, Fitch JM, Babiarz JP, Doane KJ, Linsenmayer TF: Collagen fibrillogenesis in vitro: interaction of types I and V collagen regulates fibril diameter. J Cell Sci 1990, 95:649–657
18. Wenstrup RJ, Florer JB, Brunskill EW, Bell SM, Chervoneva I, Birk DE: Type V collagen controls the initiation of collagen fibril assembly. J Biol Chem 2004, 279:53331–53337
19. Wenstrup RJ, Florer JB, Cole WG, Willing MC, Birk DE: Reduced type I collagen utilization: a pathogenic mechanism in COL5A1 haploinsufficient Ehlers-Danlos syndrome. J Cell Biochem 2004, 92:113–124
20. Wenstrup RJ, Florer JB, Davidson JM, Phillips CL, Pfeiffer BJ, Menezes DW, Chervoneva I, Birk DE: Murine model of the Ehlers-Danlos syndrome. col5a1 haploinsufficiency disrupts collagen fibril assembly at multiple stages. J Biol Chem 2006, 281:12888–12895
21. Wenstrup RJ, Smith SM, Florer JB, Zhang G, Beason DP, Seegmiller RE, Soslowsky LJ, Birk DE: Regulation of collagen fibril nucleation and initial fibril assembly involves coordinate interactions with collagens V and XI in developing tendon. J Biol Chem 2011, 286: 20455–20465
22. Sun M, Chen S, Adams SM, Florer JB, Liu H, Kao WW, Wenstrup RJ, Birk DE: Collagen V is a dominant regulator of collagen fibrillogenesis: dysfunctional regulation of structure and function in a corneal-stroma-specific Col5a1-null mouse model. J Cell Sci 2011, 124:4096–4105
23. Zhang G, Young BB, Ezura Y, Favata M, Soslowsky LJ, Chakravarti S, Birk DE: Development of tendon structure and function: regulation of collagen fibrillogenesis. J Musculoskelet Neuronal Interact 2005, 5:5–21
24. Blitz E, Viukov S, Sharir A, Shwartz Y, Galloway JL, Pryce BA, Johnson RL, Tabin CJ, Schweitzer R, Zelzer E: Bone ridge patterning during musculoskeletal assembly is mediated through SCX regulation of Bmp4 at the tendon-skeleton junction. Dev Cell 2009, 17:861–873
25. Ansorge HL, Meng X, Zhang G, Veit G, Sun M, Klement JF, Beason DP, Soslowsky LJ, Koch M, Birk DE: Type XIV collagen regulates fibrillogenesis: premature collagen fibril growth and tissue dysfunction in null mice. J Biol Chem 2009, 284:8427–8438
26. Peltz CD, Perry SM, Getz CL, Soslowsky LJ: Mechanical properties of the long-head of the biceps tendon are altered in the presence of rotator cuff tears in a rat model. J Orthop Res 2009, 27:416–420
27. Connizzo BK, Freedman BR, Fried JH, Sun M, Birk DE, Soslowsky LJ. Regulatory role for collagen V in establishing mechanical properties of tendons and ligaments is tissue dependent. J Orthop Res, In press.
28. Chen S, Oldberg A, Chakravarti S, Birk DE: Fibromodulin regulates collagen fibrillogenesis during peripheral corneal development. Dev Dyn 2010, 239:844–854
29. Brent AE, Schweitzer R, Tabin CJ: A somitic compartment of tendon progenitors. Cell 2003, 113:235–248
30. Schweitzer R, Chyung JH, Murtaugh LC, Brent AE, Rosen V, Olson EN, Lassar A, Tabin CJ: Analysis of the tendon cell fate using Scleraxis, a specific marker for tendons and ligaments. Development 2001, 128:3855–3866
31. Muzumdar MD, Tasic B, Miyamichi K, Li L, Luo L: A global double-fluorescent Cre reporter mouse. Genesis 2007, 45:593–605
32. Pritzker KP, Gay S, Jimenez SA, Ostergaard K, Pelletier JP, Revell PA, Salter D, van den Berg WB: Osteoarthritis cartilage histopathology: grading and staging. Osteoarthritis Cartilage 2006, 14:13–29
33. Elliott DH: Structure and function of mammalian tendon. Biol Rev Camb Philos Soc 1965, 40:392–421
34. Silver FH, Freeman JW, Seehra GP: Collagen self-assembly and the development of tendon mechanical properties. J Biomech 2003, 36: 1529–1553
35. Benjamin M, Ralphs JR: The cell and developmental biology of tendons and ligaments. Int Rev Cytol 2000, 196:85–130
36. Birk DE, Fitch JM, Babiarz JP, Linsenmayer TF: Collagen type I and type V are present in the same fibril in the avian corneal stroma. J Cell Biol 1988, 106:999–1008
37. Nielsen RH, Couppé C, Jensen JK, Olsen MR, Heinemeier KM, Malfait F, Symoens S, De Paepe A, Schjerling P, Magnusson SP, Remvig L, Kjaer M: Low tendon stiffness and abnormal ultrastructure distinguish classic Ehlers-Danlos syndrome from benign joint hypermobility syndrome in patients. FASEB J 2014, 28:4668–4676
38. Birk DE, Zycband E: Assembly of the tendon extracellular matrix during development. J Anat 1994, 184:457–463
39. Birk DE, Trelstad RL: Extracellular compartments in tendon morphogenesis: collagen fibril, bundle, and macroaggregate formation. J Cell Biol 1986, 103:231–240
40. Smith SM, Zhang G, Birk DE: Collagen V localizes to pericellular sites during tendon collagen fibrillogenesis. Matrix Biol 2014, 33:47–53
41. Smith SM, Thomas CE, Birk DE: Pericellular proteins of the developing mouse tendon: a proteomic analysis. Connect Tissue Res 2012, 53:2–13
42. Symoens S, Renard M, Bonod-Bidaud C, Syx D, Vaganay E, Malfait F, Ricard-Blum S, Kessler E, Van Laer L, Coucke P, Ruggiero F, De Paepe A: Identification of binding partners interacting with the alpha1-N-propeptide of type V collagen. Biochem J 2011, 433:371–381
43. Cimino F, Volk BS, Setter D: Anterior cruciate ligament injury: diagnosis, management, and prevention. Am Fam Physician 2010, 82:917–922
44. Kessler MW, Barr J, Greenwald R, Lane LB, Dines JS, Dines DM, Drakos MC, Grande DA, Chahine NO: Enhancement of Achilles tendon repair mediated by matrix metalloproteinase inhibition via systemic administration of doxycycline. J Orthop Res 2014, 32:500–506
45. Arnoczky SP, Lavagnino M, Egerbacher M, Caballero O, Gardner K: Matrix metalloproteinase inhibitors prevent a decrease in the mechanical properties of stress-deprived tendons: an in vitro experimental study. Am J Sports Med 2007, 35:763–769
46. Heath EI, Grochow LB: Clinical potential of matrix metalloprotease inhibitors in cancer therapy. Drugs 2000, 59:1043–1055
47. Fenlon D, Addington-Hall JM, O'Callaghan AC, Clough J, Nicholls P, Simmonds P: A survey of joint and muscle aches, pain, and stiffness comparing women with and without breast cancer. J Pain Symptom Manage 2013, 46:523–535